

DESIGN APPROACH FOR SUBSEA DATA CENTER BASED ON THERMODYNAMIC THEORY UNDER THE PREMISE OF BUILDING ENERGY CONSERVATION

by

**Fang LIU^{a,d}, Ya ZHAO^{a,b*}, Ligang YUAN^d, Yang ZENG^e, Caiyan ZHAI^d,
Zhuozhuang TONG^a, Juan HUANG^a, Hao LI^a, and Jiayi LIU^a**

^aSchool of Management, Hunan University of Information Technology, Changsha, China

^bSchool of Civil Engineering, Changsha University of Science and Technology, Changsha, China

^cHunan Exploration Design Research Institute, Changsha, China

^dChina Aviation Construction Engineering Co., Ltd, Changsha, China

^eUrban Rail Branch of China Railway Guangzhou Engineering Bureau Group Co., Ltd.,
Guangzhou, China

Original scientific paper

<https://doi.org/10.2298/TSCI2106209L>

Traditional data centres often require additional energy to drive air conditioning fans etc. to dissipate heat due to the serious power generation problems of servers, which in effect raises the economic costs. Seawater, with its high specific heat capacity and fluidity, offers a viable research direction for reducing economic costs, and this paper is based on this problem. The study shows that it is feasible to use containers as the main structure of the data centre. The number of servers $n \leq 860$ that can be tolerated by the cooling capacity of the container without considering the limit of geometrical constraints is obtained by calculation. Secondly, in order to enhance the heat dissipation capacity of the data centre, the 6 cm straight ribbed crown fin heat dissipation enclosure is proposed to have the best heat dissipation capacity when comparing various heat dissipation enclosure configurations. A comprehensive assessment model of material properties was established, and the weights of each straight index were determined by analytic hierarchy process, and then the metals were ranked according to the specific scores of each index. The results show that nickel alloys and aluminium alloys are the most suitable.

Key words: energy efficiency in buildings, thermodynamics, thermal design, analytic hierarchy process assessment model

Introduction

With the increasing development of technology, the 21st century has entered a new century of data. But while we enjoy the convenience of data and technology in our lives, we should also be aware of the problem of power consumption. According to statistics, 2% of the world's total annual electricity consumption is used for data centre work, which accounts for

*Corresponding author, e-mail: zhaoya900803@163.com

the majority of the IT industry's costs. Thirty percent of this consumption is used to dissipate heat from electronic devices.

Currently, most data centres in China are built inland, which not only takes up a lot of land resources, but also increases the resource consumption for cooling. As the number of data centres continues to increase, people are beginning to shift the construction of data centres from inland to the ocean.

However, the design of subsea data centres to ensure the economical dissipation of heat is currently the focus of this research. In this paper, a container is used as the main structure of the subsea data centre and the maximum capacity of the data centre is analysed based on Newton's heat transfer law and a power constraint model. An analytic hierarchy process (AHP) evaluation model is also used to determine the metal material type of the container. Finally, the seasonal and tidal influences on water mobility and temperature are analysed. The results can be used as a reference for the design of subsea data centres.

Undersea data centre capacity calculation

Computational models

The dimensions of the data centre container used for the calculations in this paper are a cylindrical shape with a diameter of 1 m and a length of 12 m, placed in suspension (the axis of the cylinder is parallel to the sea level). The theory based on thermodynamic analysis uses the following assumptions in order to simplify the analysis.

- That the container is assumed to be a single unit and that heat exchange at the interfaces is ignored.
- That the container is assumed to have a uniform internal density, *i.e.* that the container undergoes direct heat transfer with seawater.
- It is assumed that the heat transfer coefficient of the container is only influenced by the tides and seasons and is not affected by other marine activities.

Natural convection heat transfer

The flow caused by the inhomogeneity of the fluid's own temperature field is called natural convection [1]. Generally speaking, the inhomogeneous temperature field only occurs within a thin layer close to the heat transfer wall. At the wall, the fluid temperature is equal to the wall temperature, T_w , and gradually decreases in the direction of leaving the wall until the ambient temperature around, T_0 .

Consider the following theoretical and empirical equation between the heat transfer coefficient, h_i , and the Nusselt number in a transverse cylindrical model under natural convection conditions:

$$Nu = \frac{h_i d}{\lambda_{sea}} \quad (1)$$

$$Nu = C (Gr Pr)^n \quad (2)$$

where Gr is the Grashof number, λ_{sea} – the thermal conductivity of seawater, and d – the effective length of the contact surface of the study object with seawater:

$$Gr = \frac{g \beta H^3 \Delta T}{\nu^2} \quad (3)$$

where ν is the viscosity of seawater at room temperature and calculate λ_{sea} to obtain the heat transfer coefficient for side cooling under natural convection conditions. For the vertical flat plate and vertical cylinder, the characteristic length is the height, H [2]. For the horizontal cylinder in this problem, it is the external diameter, d .

Forced convection

Forced convection heat transfer refers to the heat exchange between the fluid participating in the heat transfer and the solid wall when it is driven by power or pressure head. For example, blowing electric fans, tumbling liquids in pots and pans while cooking, stirring hot soup, etc. can be considered forced convection [3].

For forced convection, this can be calculated using:

$$\frac{h_i d}{\lambda_{\text{sea}}} = C' \text{Re}^n \text{Pr}^{1/3} \quad (4)$$

$$\text{Re} = \frac{ud}{\nu} \quad (5)$$

where Re is the Reynolds factor and u – the speed of seawater flow, and if the speed of seawater cannot be measured precisely during the experiment, the range of water speed can be estimated empirically.

Capacity calculation

The analysis shows that there are two types of convective heat transfer: Natural convection and forced convection, each of which has a different heat transfer coefficient, h .

In actual seawater, the direction of the water flow is uncertain, *i.e.* there may be forced convection, so this paper uses mixed convection heat transfer for the calculation. Also due to the mixed convection that exists for both forced and natural convection [4, 5]. Therefore, it is assumed in this paper that the effect of natural convection on the total heat transfer is regarded as pure forced convection when the effect of forced convection on the total heat transfer is less than 10%; The effect of forced convection on the total heat transfer is regarded as pure natural convection when the effect of forced convection on the total heat transfer is less than 10%. The heat transfer coefficient of the seawater in Tangdao Bay of the Yellow Sea, which is more similar to the South China Sea, is selected as the reference basis [6], with $h = 597.82 \text{ W}/(\text{m}^2\text{K})$.

Based on the previous conditions, assuming that the data centre can accommodate n processors, the following constraint case needs to be satisfied.

$$\begin{aligned} n \times P_{\text{processors}} &\leq Q_{\text{Heat dissipation power}} \quad (\text{Power constraints}) \\ n \times v_{\text{processors}} &\leq v_{\text{Container}} \quad (\text{Geometric constraints}) \end{aligned} \quad (6)$$

where

$$Q_{\text{heat dissipation power}} = hS(T_w - T_0) \quad (7)$$

From the model constraints we can find:

$$n \leq 860.8608$$

As n should be rounded down, *i.e.* $n = 860$ when considering only the thermal requirements of the server.

Undersea data centre thermal design

The container heat dissipation rate and the shell of the heat dissipation capacity is proportional to the relationship, so the use of what form of heat dissipation shell on the impact of data centre heat dissipation capacity is extremely critical.

Fin type heat sink thermal analysis

Finned heat sinks [7] are the most widely used in high-power devices and are one of the most widely used enhanced heat transfer devices in engineering. There are three basic forms of fins: straight rib, ring rib and spike rib [8]. In order to maximise the heat dissipation capacity of the data centre the finned heat sink is chosen as the external structure in this paper, and its heat dissipation capacity, ϕ , can be calculated according to the fin thermal conductivity differential equation:

$$\phi = -\lambda A \frac{d\theta}{dx} \Big|_{x=0} = \lambda A \theta_0 m \cdot th(mH) = \sqrt{h_c U \lambda A} \theta_0 m \cdot th(mH) \quad (8)$$

where $th(mH)$ is the hyperbolic tangent function, calculated:

$$th(mH) = \frac{e^{mH} - e^{-mH}}{e^{mH} + e^{-mH}}$$

The thermal efficiency of fins

Fin heat dissipation efficiency [9] is defined as the ratio of the actual amount of heat dissipated by the fins to the ideal amount of heat dissipated assuming the entire fin surface is at fin root temperature. It is calculated:

$$\eta_f = \frac{\phi}{\phi_0} \quad (9)$$

where ϕ is the actual amount of heat dissipated by the fins and ϕ_0 – the ideal amount of heat dissipated by the fins, calculated according to:

$$\phi_0 = h_c U H (T_w - T_0) \quad (10)$$

Therefore, the fin efficiency of a straight fin of equal cross-section is:

$$\eta_f = \frac{\phi}{\phi_0} = \frac{\sqrt{h_c U \lambda A} \theta_0 m \cdot th(mH)}{h_c U H \theta_0} = \sqrt{\frac{\lambda A}{h_c U}} \frac{th(mH)}{H} = \frac{th(mH)}{mH} \quad (11)$$

The previous equation shows that the fin efficiency is related to the thermal conductivity, λ , the convection heat dissipation coefficient, h_c , the geometry and size of the fins, etc. As can be seen from fig. 3, when the value of mH is small η_f is higher. At a certain height, H , a smaller, m , is beneficial to increase η_f [10, 11].

The thermal structure of finned heat sinks

As the container in this paper is cylindrical and the maximum design size of the enclosure does not

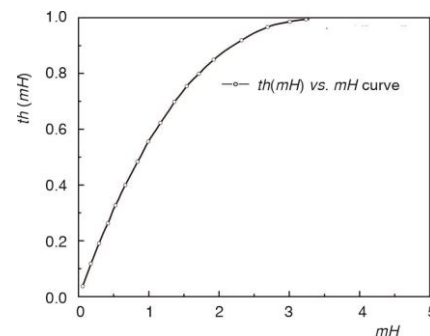


Figure 1. Values of $th(mH)$ vs. mH

exceed $1 \text{ m} \times 1 \text{ m} \times 12 \text{ m}$. The advantage of this design is that it has a smaller drag coefficient and a more stable structure while maintaining the heat dissipation capacity.

To further consider the heat dissipation capacity, the average surface heat transfer coefficient is defined:

$$\overline{ho} = \frac{\Sigma Q}{T_w - T_0} \quad (12)$$

where \overline{ho} is the average surface heat transfer coefficient and ΣQ – the heat flow density on the external surface of the finned tube (total heat transfer on the external surface of the fins and the cylinder).

As can be seen from tab. 1, the effect of changing the fin spacing on the average surface heat transfer coefficient of the finned tube is:

- When the fin spacing is within 10 cm, as the fin spacing decreases, the heat dissipation performance of the finned tube decreases and the average surface heat transfer coefficient decreases.
- When the fin spacing is above 10 cm, the heat dissipation between the fins basically does not affect each other and the average surface heat transfer coefficient basically remains the same.

Table 1. Relationship between fin pitch and heat dissipation efficiency

| Serial number | Fin spacing [cm] | Surface heat transfer coefficient |
|---------------|------------------|-----------------------------------|
| 1 | 5 | 4.71 |
| 2 | 6 | 5.58 |
| 3 | 8 | 6.60 |
| 4 | 10 | 7.12 |
| 5 | 14 | 7.45 |
| 6 | 15 | 7.45 |
| 7 | 16 | 7.38 |
| 8 | 18 | 7.45 |
| 9 | 22 | 7.68 |
| 10 | 33 | 7.42 |

The \overline{hoS} is defined to represent the overall effect of the finned tube's external surface heat dissipation performance after the fin spacing has been changed and is calculated:

$$\overline{hoS} = \frac{\Sigma Q}{T_w - T_0} \quad (13)$$

A comparison was made with a fin spacing of 10 cm and the following results were obtained in tab. 2.

Table 2. Relationship between fin spacing and the variation of each indicator

| Fin spacing [cm] | Average surface heat transfer coefficient | Surface area increment | Incremental surface heat transfer coefficient | Incremental thermal conductivity |
|------------------|---|------------------------|---|----------------------------------|
| 10 | 7.12 | 0% | 0% | 0% |
| 5 | 4.71 | 85.9% | –33.8% | 23.1% |
| 6 | 5.58 | 57.2% | –21.6% | 23.2% |
| 8 | 6.6 | 21.5% | –7.3% | 12.6% |
| 14 | 7.45 | –24.5% | 4.6% | –21.1% |
| 15 | 7.45 | –28.6% | 4.6% | –25.3% |
| 16 | 7.38 | –32.3% | 3.7% | –29.8% |
| 18 | 7.45 | –38.2% | 4.6% | –35.4% |
| 22 | 7.68 | –46.8% | 7.9% | –42.6% |
| 33 | 7.42 | –59.9% | 4.2% | –58.2% |

Based on the previous calculations, it is therefore considered that a straight ribbed crown shell with a spacing of 6 cm is optimal for the external structure of the data centre.

The AHP-based comprehensive material evaluation model

In order to quantitatively analyse the choice of materials for the subsea data centre on the basis of cost economy, this paper uses hierarchical analysis [12] for evaluation.

Evaluation factors

The selection of materials for subsea data centres is governed by several influencing factors. In this paper, pressure resistance, corrosion resistance, metal price, processing cost and thermal conductivity are mainly considered as the basis for evaluation. Based on the comprehensive consideration, five types of materials, namely aluminium alloys, copper alloys, nickel alloys, titanium alloys and fine steel, are selected as the main evaluation objects.

Indicator weights

The weights, W , are used to describe the relative importance of each evaluation indicator for the purpose of the assessment. The set of weights is a multi-level set corresponding to the set of evaluation factors, *i.e.* $\omega = (\omega_1, \omega_2, \omega_3, \omega_4, \omega_5)$. In this paper, the weight calculation problem is decomposed into two levels, and the AHP evaluation model is constructed:

- The uppermost level is the target level M , *i.e.* assessing the overall performance of a material.
- The lowermost level is the benchmark level, *i.e.* individual indicators $C1-C5$.

Construct the judgment matrix $M-C$: compare the five elements in the base layer two by two to obtain the comparison matrix, as shown in tab. 3.

Table 3. Comparison matrix

| M | C1 | C2 | C3 | C4 | C5 |
|----|-------|------|------|------|------|
| C1 | 1.00 | 0.80 | 1.20 | 1.40 | 0.70 |
| C2 | 1.30 | 1.00 | 1.20 | 1.30 | 1.10 |
| C3 | 1/1.2 | 0.83 | 1.00 | 1.10 | 0.80 |
| C4 | 0.77 | 0.77 | 0.91 | 1.00 | 0.80 |
| C5 | 1.43 | 0.91 | 1.25 | 1.25 | 1.00 |

Solving for the eigenvalues of $M-C$ yields $\lambda = 5.0434$ and the weights are:

$$W = [0.1950 \ 0.2318 \ 0.1789 \ 0.1668 \ 0.2275].$$

From the formula $CI = (\lambda_{\max} - n)/(n - 1)$ so according to $CR = CI/RI$ we got $CR = 0.0108 < 0.1$ which passed the consistency test.

The CR_j values for matrices $C1-P$, $C2-P$, $C3-P$, $C4-P$, and $C5-P$ were calculated to pass the consistency test. The final summary results of the total weights were determined as shown in tab. 4.

Table 4. Weighting of the indicators

| Indicator name | Weighting |
|----------------------|-----------|
| Pressure resistance | 0.1950 |
| Corrosion resistance | 0.2318 |
| Metal prices | 0.1789 |
| Processing costs | 0.1668 |
| Thermal conductivity | 0.2275 |

Material performance assessment models

The following material performance assessment model is established. Let G_i denote the assessment score of the material in i , where $\omega_1, \omega_2, \omega_3, \omega_4, \omega_5$ denote the weights of the five indicators respectively, and a_i, b_i, c_i, d_i, e_i denote the individual indicator scores of the i^{th} material:

$$G_i = \omega_1 a_i + \omega_2 b_i + \omega_3 c_i + \omega_4 d_i + \omega_5 e_i \quad (14)$$

As different indicators have different magnitudes, their indicators need to be normalised by transforming the series x_1, x_2, \dots, x_n :

$$y_i = \frac{x_i - \min(x_j)}{\max(x_j) - \min(x_j)} \quad (15)$$

Then the new sequence $y_1, y_2, \dots, y_n \in [0,1]$ and is dimensionless.

Refer to tab. 5 for data on price, hardness, metal activity, modulus of elasticity and thermal conductivity of the different materials.

Table 5. Data for each indicator

| Name of material | Price (Yuan per tonne) | Hardness (machining difficulty) | Metal activity | Modulus of elasticity | Thermal conductivity W/(mk) |
|------------------|---------------------------|------------------------------------|-------------------|--------------------------|--------------------------------|
| Aluminium | 18130 | 31 | 5 | 10×10^6 | 209 |
| Copper alloys | 68550 | 50 | 1 | 17×10^6 | 109 |
| Nickel alloys | 123850 | 90-130 | 2 | 26×10^6 | 82.57 |
| Titanium | 2425 | 90 | 4 | 16.5×10^6 | 15.24 |
| Steel | 17000 | 75 | 3 | 30×10^6 | 16.2 |

The data were normalised and the normalised data were as shown in tab. 6.

Table 6. Standardised indicator data

| Name of material | a_i | b_i | c_i | d_i | e_i |
|------------------|--------|--------|--------|--------|--------|
| Aluminium | 0.5260 | 0.3959 | 0.0000 | 0.2114 | 0.8335 |
| Copper alloys | 0.2751 | 0.2684 | 0.7303 | 0.3594 | 0.4347 |
| Nickel alloys | 0.0000 | 0.8724 | 0.5477 | 0.5497 | 0.3293 |
| Titanium | 0.6041 | 0.0000 | 0.1826 | 0.3488 | 0.0608 |
| Steel | 0.5260 | 0.3959 | 0.0000 | 0.2114 | 0.8335 |

Substituting into eq. (14), the final score is obtained as in tab. 7.

Table 7. Final scores for different materials

| Name of material | Overall score |
|------------------|---------------|
| Aluminium | 0.2288 |
| Copper alloys | 0.2189 |
| Nickel alloys | 0.2520 |
| Titanium | 0.1362 |
| Steel | 0.1641 |

Table 7 shows that nickel alloys score highest, are easy to work with and have a high resistance to compression, but are slightly more expensive. Aluminium has a slightly lower score, although it is slightly less resistant to corrosion but has a clear price advantage and is more thermally conductive. Therefore, nickel alloy is recommended as the housing material if there is enough money for construction, while aluminium alloy is recommended in the opposite direction.

Conclusion

- The use of a cylindrical container as a subsea data centre is feasible. A power constraint model was developed based on Newton's heat transfer law using a mixed convection heat transfer coefficient of $h = 597.82 \text{ W/(m}^2\text{K)}$: $n \times P_{\text{processors}} \leq Q_{\text{heat dissipation power}}$. By calculating the number of servers $n \leq 860$ that can be tolerated by the cooling capacity of the container without considering the limit of geometric constraints.
- The thermal capacity of subsea data centres is controlled by the external structure. The calculations in this paper show that a straight ribbed crown fin heat sink enclosure with a pitch of 6 cm can ensure the heat sink efficiency of the data centre.
- The selection of data centre enclosure materials requires consideration of the influence of various factors. This paper determines the weights of each indicator by establishing an AHP evaluation model, and the results show that nickel alloy and aluminium alloy are the most suitable.

References

- [1] Li, J., Optimization of a Phase Change Heat Storage Device Based on Natural Convection, M. Sc. thesis, Guangzhou University, Guangzhou, China, 2020
- [2] Zhao, X. J., et al., Matching Model of Energy Supply and Demand of the Integrated Energy System in Coastal Areas, *Journal of Coastal Research*, 103 (2020), sp1, 983
- [3] Wang, Q., Synergistic Analysis of Convective Heat Transfer Fields in Electric Field-Enhanced Heat Transfer Tubes, M. Sc. thesis, Northeast Electric Power University, Jilin, China, 2020
- [4] Yu, D., et al., A New LQG Optimal Control Strategy Applied on a Hybrid Wind Turbine/Solid Oxide Fuel Cell/ in the Presence of the Interval Uncertainties, *Sustainable Energy, Grids and Networks*, 21 (2020), Mar., 100296
- [5] He, L., et al., A Three-Level Framework for Balancing the Tradeoffs Among the Energy, Water, and Air-Emission Implications Within the Life-Cycle Shale Gas Supply Chains, *Resources, Conservation and Recycling*, 133 (2018), June, pp. 206-228
- [6] Li, X. C., Study on the Flow and Heat Transfer Law of Low Temperature Seawater Out-Swept Circular Tube, M. Sc. thesis, China University of Petroleum (East China), Qingdao, China, 2017
- [7] Yang, J. S., Numerical Simulation of Heat Transfer Enhancement of Air-Cooled Heat Sinks for Electronic Devices, M. Sc. thesis, Huazhong University of Science and Technology, Wuhan, China, 2019
- [8] Li, J., et al., Structural Analysis and Optimization of Finned Heat Sinks For High Power LED Lamps (in Chinese), *China Light & Lighting*, 3 (2016), pp. 33-36
- [9] Cao, L. L., Simulation and Optimization of the Thermal Performance of Centrifugal CPU Coolers, M. Sc. thesis, University of South China, Hengyang, China, 2020
- [10] He, L., et al., Ecological Vulnerability Assessment for Ecological Conservation and Environmental Management, *Journal of Environmental Management*, 206 (2018), Jan., pp. 1115-1125
- [11] Yang, C., et al., Energy Efficiency Modeling of Integrated Energy System in Coastal Areas, *Journal of Coastal Research*, 103 (2020), sp1, 995
- [12] Si, S. K. *Mathematical Modelling Algorithms and Applications*, National Defense Industry Press, Beijing, China, 2011